Protein Synthesis, Post-Translation Modification, and Degradation:

Tripeptide Mimetics Inhibit the 20 S Proteasome by Covalent Bonding to the Active Threonines

Hannes A. Braun, Sumaira Umbreen, Michael Groll, Ulrike Kuckelkorn, Izabela Mlynarczuk, Moritz E. Wigand, Ilse Drung, Peter-Michael Kloetzel and Boris Schmidt

J. Biol. Chem. 2005, 280:28394-28401.
doi: 10.1074/jbc.M502453200 originally published online May 26, 2005

THE JOURNAL OF BIOLOGICAL CHEMISTRY
Vol. 280, No. 31, Issue of August 5, pp. 28394–28411, 2005
Printed in U.S.A.

Tripeptide Mimetics Inhibit the 20 S Proteasome by Covalent Bonding to the Active Threonines*

Received for publication, March 4, 2005, and in revised form, May 25, 2005
Published, JBC Papers in Press, May 26, 2005, DOI 10.1074/jbc.M502453200

Hannes A. Braun‡, Sumaira Umbreen‡, Michael Groll§, Ulrike Kuckelkorn¶, Izabela Mlynarczuk¶‖, Moritz E. Wigand¶, Ilse Drung¶, Peter-Michael Kloetzel¶, and Boris Schmidt‡

From the ‡Darmstadt University of Technology, Clemens Schöpf-Institute for Organic Chemistry and Biochemistry, D-64287 Darmstadt, Germany, §Institute for Physiological Chemistry, Ludwig Maximilian University München, D-81377 Munich, Germany, ¶Charité-Universitätsmedizin Berlin, Institute for Biochemistry, D-10117 Berlin, Germany, and ‖Department of Histology and Embryology, Center of Biostructure Research, The Medical University of Warsaw, 02-004 Warsaw, Poland

Proteasomes play an important role in protein turnover in living cells. The inhibition of proteasomes affects cell cycle processes and induces apoptosis. Thus, 20 S proteasomal inhibitors are potential tools for the modulation of neoplastic growth. Based on MG132, a potent but nonspecific 20 S proteasome inhibitor, we designed and synthesized 22 compounds and evaluated them for the inhibition of proteasomes. The majority of the synthesized compounds reduced the hydrolysis of LLVY-7-aminomethylcoumarin peptide substrate in cell lysates, some of them drastically. Several compounds displayed inhibitory effects when tested *in vitro* on isolated 20 S proteasomes, with lowest IC_{50} values of 58 nM (chymotrypsin-like activity), 53 nM (trypsin-like activity), and 100 nM (caspase-like activity). Compounds 16, 21, 22, and 28 affected the chymotrypsin-like activity of the β5 subunit exclusively, whereas compounds 7 and 8 inhibited the β2 trypsin-like active site selectively. Compounds 13 and 15 inhibited all three proteolytic activities. Compound 15 was shown to interact with the active site by x-ray crystallography. The potential of these novel inhibitors was assessed by cellular tolerance and biological response. HeLa cells tolerated up to 1 μM concentrations of all substances. Intracellular reduction of proteasomal activity and accumulation of polyubiquitinated proteins were observed for compounds 7, 13, 15, 22, 25, 26, 27, and 28 on HeLa cells. Four of these compounds (7, 15, 26, and 28) induced apoptosis in HeLa cells and thus are considered as promising leads for antitumor drug development.

The balance of protein synthesis and degradation processes is essential to maintain cellular homeostasis. Cells possess two major pathways to fulfill protein degradation: proteins are digested either by proteolytic enzymes within the lysosomes or via the ubiquitin-proteasome system. The imbalance of the protein synthesis and degradation processes causes many pathological processes (1).

26 S proteasomes, multi-subunit protease complexes, perform ATP-dependent degradation of polyubiquitinated proteins and are responsible for most of the non-lysosomal proteolysis in eukaryotic cells. They consist of the proteolytic 20 S proteasome core particle and are capped at one or both ends by 19 S regulatory particles (2, 3). The 20 S core particle is a cylindrical assembly of 28 subunits arranged in four stacked heptameric rings; two rings are formed by 7 α-type subunits, and two rings are build of 7 β-type subunits (4, 5). The two inner β-rings form the central cavity of the cylinder and harbor the proteolytic sites. In contrast to prokaryotic 20 S proteasomes, which contain 14 identical proteolytically active β-type subunits, eukaryotic 20 S proteasomes belong to the family of N-terminal nucleophilic hydrolases (6, 7). They possess only three subunits with N-terminal active site threonines in the β-ring. In addition, the stimulation of mammalian cells by γ-interferon causes the replacement of the three active β-subunits β1, β2, and β5 by their immunohomologues β1i, β2i, and β5i, resulting in the formation of immunoproteasomes, which display modified cleavage patterns of substrate peptides. The functional integrity of proteasomes is indispensable for a variety of cellular functions, such as metabolic adaptation, cell differentiation, cell cycle control, stress response, degradation of abnormal proteins, and generation of epitopes presented by major histocompatibility complex class I receptors (for reviews, see Refs. 8 and 9). However, proteasomes are an important supplier (but not the exclusive supplier) of antigenic peptides (10, 11).

The deregulation of the ubiquitin-proteasome protein degradation pathway in humans causes several diseases, such as cancer and neurodegenerative, autoimmune, and metabolic disorders. Inhibition of proteasomes influences the stability of many proteins, especially those that are involved in the cell cycle regulation. In fact, most of the cells treated with proteasomal inhibitors become sensitive to apoptosis (12, 13). Thus, selective inhibitors of catalytic proteasome subunits are attractive targets for drug development (14). Interestingly, tumor cells are usually more sensitive to proteasomal inhibition than normal cells. Healthy cells display cell cycle arrest when treated with proteasomal inhibitors but, in contrast to tumor cells, are not as susceptible to apoptosis (15, 16). So far, several proteasomal inhibitors have been characterized, both selective (**4**, lactacystin; **5**, TMC-95A; and **6**, epoxomicin) and nonspecific (**1**, dichlorovinyl ester; **3**, MG132) (Fig. 1*A*) (17).

The most prominent proteasomal inhibitor **2** (Bortezomib®, VELCADE™) is approved by the United States Food and Drug Administration as a prescription drug for the treatment of multiple myeloma (18–20). Similar applications of proteasomal

* This work was supported by the Fonds der Chemischen Industrie, Deutsche Forschungsgemeinschaft Grants SPP1085 SCHM1012-3 and Ku1261, and EU Contract LSHM-CT-2003-503330 (APOPIS). The costs of publication of this article were defrayed in part by the payment of page charges. This article must therefore be hereby marked "*advertisement*" in accordance with 18 U.S.C. Section 1734 solely to indicate this fact.

** To whom correspondence should be addressed: Darmstadt University of Technology, Clemens Schöpf-Institute for Organic Chemistry and Biochemistry, Petersenstrasse 22, D-64287 Darmstadt, Germany. Tel.: 49-6151-16-3075; Fax: 49-6151-16-3278; E-mail: schmibo@oc.chemie.tu-darmstadt.de.

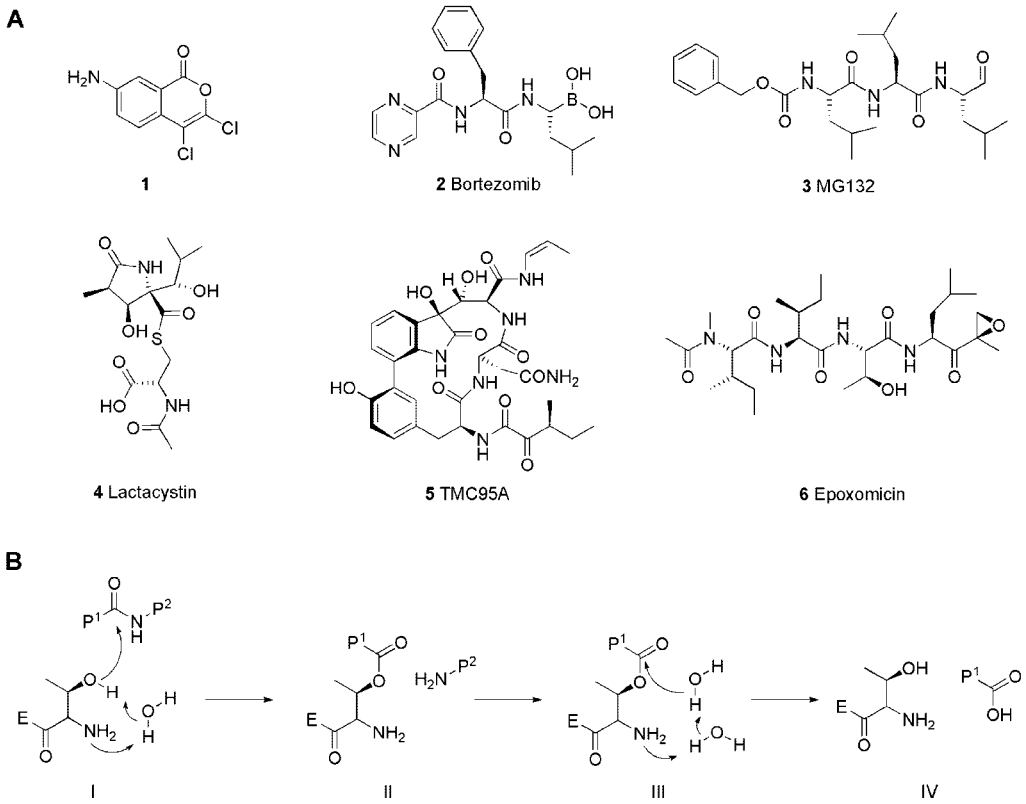

FIG. 1. *A*, serine and threonine protease inhibitors. *B*, hydrolysis by threonine proteases.

inhibitors in oncology and neurodegenerative diseases are at the focus of our interest (21). We intend to develop selective inhibitors for the three different proteolytic activities of the 20 S proteasome. Our goals may be achieved by creating compounds or reactive moieties, which bind covalently to the N-terminal threonine.

The proteasomal amide hydrolysis differs from all other classes of proteases and is performed by N-terminal threonines, as depicted in Fig. 1*B*. The crystal structure analysis of the 20 S proteasome revealed that the Thr-1Oγ functions as the nucleophile and that the N-terminal amino group serves as an acyl carrier (6). Covalent inhibitors can bind to the active site through the Thr-1Oγ hydroxyl group or both the free N terminus and Thr-1Oγ (for review, see Ref. 17).

Effective *in vivo* inhibitors of the 20 S proteasome require high selectivity and good penetration of the cellular membranes. We decided to address the selectivity problems of **3** (MG132) first. A focused set of peptide analogue aldehydes **13–18** aimed at the proteolytic activity of β5 subunit was synthesized and tested for inhibition of the 20 S proteasome and β-secretase (22, 23). These results encouraged us to address the design of irreversible and selective proteasome inhibitors. We concentrated on the nonspecific serine protease inhibitor **1** and introduced modifications to improve its selective inhibition of the chymotrypsin-like activity of the 20 S proteasome.

MATERIALS AND METHODS

Isolation of 20 S Proteasomes—20 S proteasomes were isolated from red blood cells. Cells were lysed with dithiothreitol (1 mM), and the stroma-free supernatant was applied to DEAE-Sepharose (Toyopearls). 20 S proteasome was eluted with a NaCl gradient in TEAD (20 mM Tris-HCl, pH 7.4, 1 mM EDTA, 1 mM azide, and 1 mM dithiothreitol) from 100 to 350 mM NaCl. 20 S proteasome was concentrated by ammonium sulfate precipitation (between 40 and 70% of saturation) and separated in a 10–40% sucrose gradient by centrifugation at 40,000 rpm for 16 h (SW40; L7; Beckman & Coulter). Finally, 20 S proteasome was purified on MonoQ column and eluted with a NaCl gradient at 280 mM NaCl. The fractions containing purified 20 S proteasome were dialyzed against 50 mM NaCl in TEAD and stored on ice. The purity was determined by SDS-PAGE.

Protease Assays—Suc-LLVY-AMC,[1] Z-VGR-AMC, and LLE-AMC (Bachem, Calbiochem) were used to estimate chymotrypsin-like, trypsin-like, and caspase-like (post-acidic) activities of the 20 S proteasome, respectively. Substrates were incubated with 20 S proteasome at 37 °C in assay buffer (20 mM Tris-HCl, pH 7.2, 1 mM EDTA, and 1 mM dithiothreitol) for 1 h. 100 ng of 20 S proteasome was preincubated with 0.01–10 μM of the inhibitors for 15 min. The reaction was started by addition of substrate (50 μM). The released AMC was detected by fluorescence emission at 460 nm (excitation at 390 nm) using a TECAN fluorometer. Activity was estimated in fluorescence units, and the inhibition is represented by IC_{50} values.

Cell Culture—HeLa cells and MeWo cells (human melanoma) were cultured in RPMI 1640 supplemented with 10% heat-inactivated fetal calf serum and penicillin/streptomycin at 5% CO_2. Inhibitors were applied from 100× stocks (in Me_2SO) at the indicated final concentrations and incubated for variable times.

Sensitivity of Cells against Added Compounds—The viability of HeLa cells was tested by crystal violet staining after incubation with inhibitors. The cells were washed once with PBS, fixed with 1% of glutardialdehyde for 30 min, and washed again. Finally, the fixed cells were stained with 0.1% crystal violet in PBS for 30 min and subsequently washed carefully with water to remove unbound dye. The remaining dye was eluted by 0.1% Triton X-100 in PBS and determined at 550 nm.

Inhibition of 20 S Proteasomes within Cells—Cells were harvested and lysed with 0.1% Nonidet P-40 in TEAD in the presence of the commercial protease inhibitor mixture Complete (Roche Applied Science). The proteasomal activity was measured in 10 μl of lysates by using Suc-LLVY-AMC as a substrate. The protein content was quantified by Bradford (Protein assay; Bio-Rad).

Detection of Accumulated Polyubiquitinated Proteins—50 μg of total cell lysate was separated by SDS-PAGE and blotted onto polyvinylidene difluoride membrane (Millipore). Blots were blocked by 5% of milk suspension. The polyubiquitinated proteins were detected by anti-ubiq-

[1] The abbreviations used are: AMC, 7-aminomethylcoumarin; Z, benzyloxycarbonyl; PBS, phosphate-buffered saline.

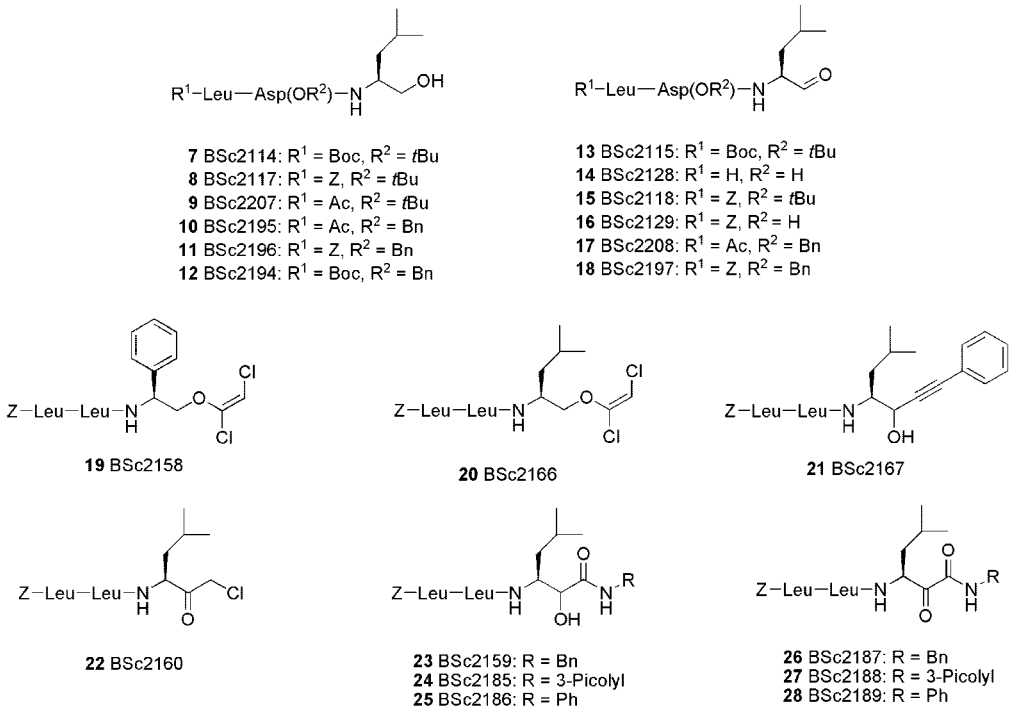

FIG. 2. **Peptidomimetics designed for 20 S proteasome inhibition.**

uitin antibody (DAKO) and anti-rabbit peroxidase-labeled as secondary antibody (DIANOVA) and then visualized by ECL.

Analysis of Cell Cycle—MeWo cells were treated with inhibitor **15** and MG132 for 24 h. Cells were trypsinized, washed with cold PBS, suspended in 70% ethanol, and fixed at −20 °C for 2 h. Fixed cells were washed twice with PBS, incubated with RNase A (Sigma) at room temperature for 20 min, and placed on ice. Propidium iodide was added to a final concentration of 5 μg/ml, and cells were stained at least for 2 h at 4 °C. The cells were analyzed after staining by flow cytometry (FACSCalibur flow cytometer; BD Biosciences) using CellQuest software. Statistical significance was determined by the χ^2 test.

Apoptosis Assay—HeLa cells (10,000 cells/well) were disseminated in a 96-well plate and treated with 1 μM of inhibitors for 20 h. The ongoing apoptosis was estimated by the Apo-One® assay (Promega).

Co-crystallization—Crystals of 20 S proteasome from *Saccharomyces cerevisiae* were grown in hanging drops at 24 °C as described previously (6) and incubated for 60 min with compound **15**. The protein concentration used for crystallization was 40 mg/ml in Tris-HCl (10 mM, pH 7.5) and EDTA (1 mM). The drops contained 3 μl of protein and 2 μl of the reservoir solution, which contained 30 mM magnesium acetate, 100 mM morpholinoethanesulfonic acid, pH 7.2, and 10% 2-methylpentane-2,4-diol.

The space group belongs to $P2_1$ with cell dimensions of a = 135.8 Å, b = 300.1 Å, c = 144.4 Å, and β = 113.1°. Data to 2.8 Å were collected using synchrotron radiation with λ = 1.05 Å on the BW6-beamline at DESY (Hamburg, Germany). Crystals were soaked in a cryoprotecting buffer (30% 2-methylpentane-2,4-diol, 20 mM magnesium acetate, 100 mM morpholinoethanesulfonic acid, pH 6.9) and frozen in a stream of liquid nitrogen gas at 90 K (Oxford Cryo Systems). X-ray intensities were evaluated by using the MOSFILM program package (version 6.1), and data reduction was performed with CCP4 (24). The anisotropy of diffraction was corrected by an overall anisotropic temperature factor by comparing observed and calculated structure amplitudes using the program X-PLOR (25). A total of 2,383,416 reflections yielding 248,616 unique reflections (96.9% completeness) was collected. The corresponding R_{merge} was 8.7% at 2.8 Å resolution (41.9% for the last resolution shell). Electron density was improved by averaging and back-transforming the reflections 10 times over the 2-fold noncrystallographic symmetry axis using the program package MAIN (26). Conventional crystallographic rigid body, positional, and temperature factor refinements were carried out with X-PLOR using the yeast 20 S proteasome structure as starting model (6). For model building, the program MAIN was used. The structure was refined to a R-factor of 21.7% (free R-factor, 24.9%) with root mean square deviations from target values of 0.007 Å for bonds and 1.30° for angles (27). Modeling experiments were performed using the coordinates of yeast 20 S proteasome with the program MAIN (26).

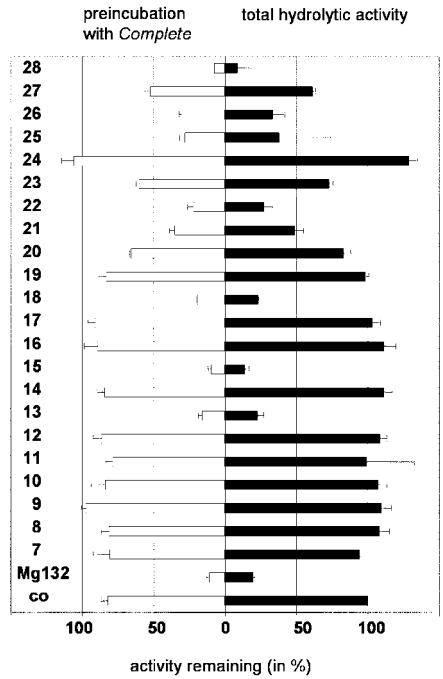

FIG. 3. **Estimation of proteolysis in cell lysates by addition of MG132 and 7–28.** Compounds (10 μM) were added to clarified lysates and preincubated for 30 min on ice prior to the proteolysis assay (*black bars*). In parallel, lysate was preincubated with the commercial protease inhibitor mixture Complete for 30 min, which inhibited most of the cytosolic serine/aspartate proteases, but not proteasomes (*white bars*). This partial inactivation was followed by incubation with the indicated compounds. The proteolytic activity was determined in 10 μl of the lysates by addition of LLVY-AMC (100 μl, 50 μM) in TEAD. The AMC released by non-inhibited lysate was set to 100%. MG132 was used as inhibition control.

Synthesis—Compounds **7–18** were synthesized as analogues of **3** (MG132) based on the established substrate preferences of β-secretase (23) by standard methodology or as published previously (28). The condensation of commercial protected dipeptides and amino acids with

TABLE I
Calculated IC_{50} values for compounds **7–28.**

IC_{50} values were calculated from inhibition of proteasomes at increasing amounts of inhibitors. Samples were preincubated for 15 min in ice. The assay was started by addition of 50 μM fluorogenic peptide substrate. LLVY-AMC and GLL-AMC for chymotryptic-like, VGR-AMC for tryptic-like, and LLE-AMC for caspase-like activity. The release of AMC was determined at 460 nm emission (excitation, 390 nm). Calculated IC_{50} values for MG132 served as controls.

Inhibitor	Access no.	IC_{50}			
		β5 Chymotrypsin-like (Y)	β5 Ch-I (L)	β2 Trypsin-like (R)	β1 Caspase-like (E)
		μM	μM	μM	μM
7	BSc2114	>10	–[a]	0.053	>10
8	BSc2117	>10	–	5.481	>10
9	BSc2207	>10	–	–	–
10	BSc2195	>10	–	–	–
11	BSc2196	>10	–	–	–
12	BSc2194	>10	–	–	–
13	BSc2115	0.382	0.102	0.495	0.098
14	BSc2128	>10	>10	>10	>10
15	BSc2118	0.058	0.031	0.155	1.791
16	BSc2129	7.26	–	>10	>10
17	BSc2208	–	–	–	–
18	BSc2197	1.731	–	–	3.122
19	BSc2158	–	–	–	–
20	BSc2166	>10		>10	>10
21	BSc2167	1.303	>10	–	–
22	BSc2160	2.196	–	–	–
23	BSc2159	–	–	–	–
24	BSc2185	–	–	–	–
25	BSc2186	0.981		–	4.04
26	BSc2187	0.441		–	1.72
27	BSc2188	0.350		–	7.966
28	BSc2189	0.072		–	>10
3	MG132	0.0242	2.240	9.215	2.288

[a] –, no inhibition.

commercial amino alcohols was followed by oxidation to the aldehydes by 2-iodooxybenzoic acid in Me_2SO.

RESULTS

The intermediate alcohol derivatives **7–12** and the tripeptidic aldehydes **13–18** were investigated for enzyme inhibition. Inhibition of β-secretase was rather poor ($IC_{50} \gg 200$ μM),[2] but several compounds turned out to be potent inhibitors of the 20 S proteasome. Peptide aldehydes generally lack selectivity in enzyme inhibition. Therefore, other moieties were tested for their ability to inhibit threonine proteases. The nonselective dichlorovinyl ester **1,** which reacts readily with all sorts of nucleophiles such as cysteine, serine, and, eventually, threonine, served as our lead, but we intended to reduce the inherent overactivation. The removal of the acyl group may reduce the nonspecific hydrolysis by ubiquitous nucleophiles and results in reasonably stable dichlorovinyl ethers (28). Such ethers (**19** and **20**) tolerate acidic environment but hydrolyze readily at pH 11 to be converted into α-chloroacetates, which in turn may react with nucleophiles. This dual reactivity, which is delivered in a cascade reaction, meets the specific requirements of an N-terminal threonine protease inhibitor. An analogue dual reactivity may be observed for propargylic ketones. A similar compound was synthesized, but unfortunately, the alcohol **21** resisted oxidation to the desired ketone. Therefore, we focused on transition state mimetics as inhibitors. Lead structures, such as statines (34), α-ketoamides, and chloromethyl ketones, are well established in protease inhibition. Combination of these structures with a β5 selective tripeptide furnished the compounds **22–28** (Fig. 2). Compound **22** was prepared from commercial Z-LL and chloromethyl leucine. Compounds **23–25** were obtained by a Passerini reaction of MG132 with three isonitriles. The subsequent oxidation by 2-iodooxybenzoic acid in Me_2SO furnished the α-ketoamides **26–28**.

All peptide mimetics (**7–28**) were tested for their ability to inhibit the 20 S proteasome. Initially, we investigated the inhibition of cellular soluble proteases. 10 μM solutions of compounds **7–28** were added to the cytosolic fraction of HeLa cells and incubated for 30 min on ice. Subsequently, the proteolytic process was monitored by addition of the peptidic substrate Suc-LLVY-AMC. In parallel, the cytosolic fraction was treated with the broad specific protease inhibitor mixture Complete (Roche Applied Science) prior to the addition of substrate. This inhibitor mixture did not affect 20 S proteasomes. 11 of 22 investigated compounds diminished proteolysis in the cytosolic fraction as well as in the Complete-pretreated lysate (Fig. 3). The inhibition rates differed drastically. Some of the compounds displayed no inhibition, whereas five of the analyzed compounds decreased the hydrolysis of Suc-LLVY-AMC by >75%.

To ensure that the inhibitory effect observed in the cytosolic fraction was indeed caused by inhibition of 20 S proteasomes, the inhibitors were added at different concentrations to isolated 20 S proteasomes. The effect of the inhibitors was compared with that of the frequently employed 20 S proteasome inhibitor **3** (MG132). The chymotryptic-like (Suc-LLVY-AMC), tryptic-like (Bz-VGR-AMC), and caspase-like (Z-LLE-AMC) activities of 20 S proteasomes were determined after incubation at 37 °C for 1 h. The strongest inhibitory effects were observed for chymotryptic-like activity. Six of the tested inhibitors (**13**, **15**, **25**, **26**, **27**, and **28**) displayed IC_{50} values of <1 μM. The inhibition of tryptic-like activity was <1 μM for the inhibitors **7**, **13**, and **15**. Only compounds **7** and **8** showed exclusive inhibition of tryptic-like activity. The inhibition of caspase-like activity was even weaker (Table I). 20 S proteasomes isolated from HeLa cells contain more constitutive proteasomes than immunoproteasomes. Therefore, we repeated the inhibition experiments with immunoproteasomes isolated from stably transfected T2.27 cells. These experiments revealed that immunoproteasomes and constitutive proteasomes display similar sensitivities to the inhibitors (data not shown). 26 S proteasomes are responsible for ATP-dependent degradation of

[2] M. Willem, S. Umbreen, and B. Schmidt, unpublished results.

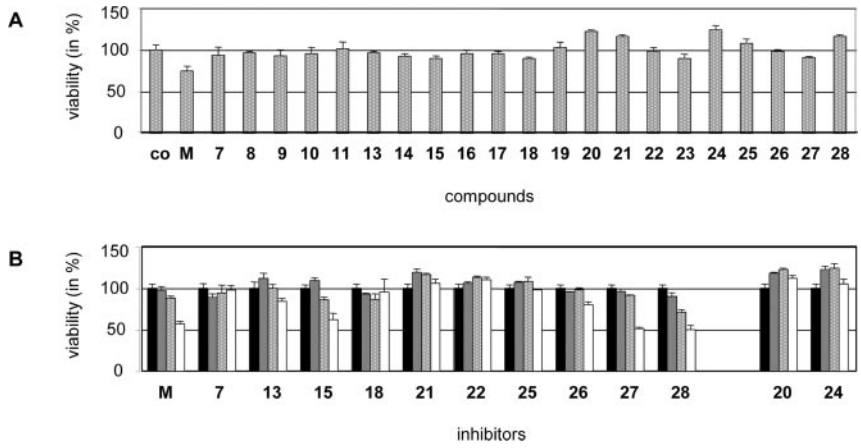

FIG. 4. *A*, viability of HeLa cells after incubation with MG132 and **7–28**. The viability of HeLa cells incubated with inhibitors (1 μM) was determined by crystal violet staining after 20 h. *B*, the viability of HeLa cells is dependent on inhibitor concentrations. HeLa cells were cultured in the presence of increasing concentrations (100 nM, *gray bars*; 1 μM, *white dotted bars*; 10 μM, *white bars*) of inhibitors for 20 h. Control cells are indicated by *black bars*. Cell survival was determined by crystal violet staining.

polyubiquitin-tagged proteins within living cells. They exhibited a similar susceptibility to the most potent inhibitor (**15**) *in vitro* (data not shown).

Protease inhibitors are often very toxic for organisms or single cells (1). Therefore, selected inhibitors were tested on cell cultures for cell lysis or cell death. The viability of HeLa cells in the presence of different compounds was tested in 24-h cultures. HeLa cells tolerated 1 μM concentrations of inhibitory and non-inhibitory substances (Fig. 4*A*). The relative survival rate of the cells was clearly diminished at concentrations of 10 μM. This effect was pronounced for the most potent inhibitors from the *in vitro* experiments (**15**, **28**, and **27**) (Fig. 4*B*).

The impact of inhibitors on living cells and organisms crucially depends on adequate cell permeability. Therefore, we analyzed the proteasome function within cells at different inhibitor concentrations. The application to cell cultures or animals required the concentrations of the inhibitors to be as low as possible. The specific proteasome activity was reduced below 50% (Fig. 5*A*) in cells treated with 1 μM solutions of **15**, **22**, **25**, **26**, and **28**. Compounds **7**, **13**, and **27** exhibited weaker effects on the specific activity, whereas compounds **18** and **21** hardly inhibited the cellular proteasome at all. Remarkably, inhibitors **15**, **22**, and **28** reduced the proteolytic activity already at a concentration of 100 nM (Fig. 5*A*). Specific inhibition of proteasomes results in the accumulation of polyubiquitinated proteins. Indeed, the amounts of polyubiquitinated proteins increased during incubation with the inhibitors. First effects were observed after 2 h for the potent compound **15** (Fig. 5*B*) and for compounds **20**, **22**, **25**, and **28** (data not shown). The accumulation of polyubiquitinated proteins via proteasome inhibition depended strongly on the applied concentrations (Fig. 5*C*). Thus, several of these new inhibitors are able to permeate cells and affect the activity of proteasomes. The consequences of proteasome inhibition for distinct cellular functions are subject to ongoing investigations.

The particular sensitivity of tumor cells to proteasome inhibitors (1) was evaluated in the melanoma cell line MeWo at different concentrations of compound **15** for 72 h. The viability was compared with MeWo cells treated with MG132 under the same conditions (Fig. 6*A*). 50% of the MeWo cells treated with 35 nM MG132 were still alive after 72 h. Very few cells survived the treatment with inhibitor **15**, which demonstrated its potency. Proteasome inhibitors can induce a cell cycle arrest in the G_1/S or G_2 phase, therefore the cell cycle progress was analyzed after 24-h inhibitor treatment of MeWo cells (Fig. 6, *B* and *C*). Compound **15** led to a cell cycle arrest in the G_2 phase, like MG132, albeit at considerably lower concentrations.

Proteasomes determine the delicate balance of life and death of the cells by controlling transcription factors and proteins involved in apoptosis. The reduction of proteasomal capacity

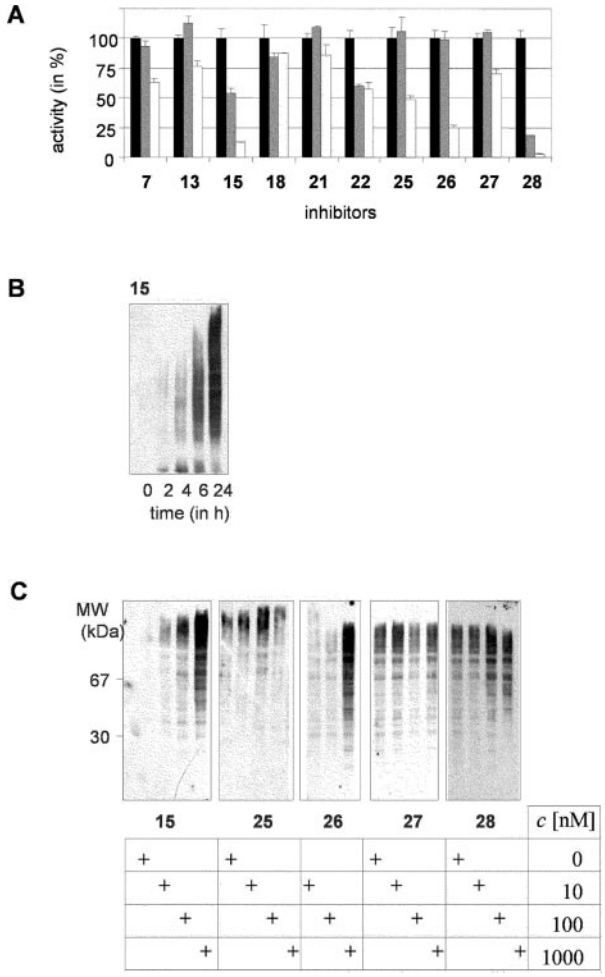

FIG. 5. **Inhibition of proteasomes within cells.** The proteasome activity and intracellular accumulation of polyubiquitinated proteins in cells co-cultured with inhibitors were tested in lysed cells. *A*, HeLa cells were cultured in the presence of inhibitors for 24 h. After lysis of cells, the protein concentration was measured according to Bradford to normalize the different cell amounts. Thereafter, Complete (Roche Applied Science) was added to all lysates, and the proteasomal activity was determined by hydrolysis of Suc-LLVY-AMC. Lysates of HeLa cells cultured without inhibitors served as control (*black bars*) and were compared with cell lysates cultivated at 100 nM (*gray bars*) and 1 μM (*white bars*). *B*, HeLa cells were cultured with 1 μM compound **15** for 2, 4, 6, and 24 h. Cells were lysed, and proteins were separated by SDS-PAGE in a 10% gel, blotted onto a polyvinylidene difluoride membrane, and detected in Western blot by an anti-ubiquitin antibody (DAKO). *C*, HeLa cells were treated with increasing concentrations of the inhibitors **15**, **25**, **26**, **27**, and **28** for 24 h (*c*, inhibitor concentration). Cells were lysed, proteins were separated in 15% gels, and the accumulation of polyubiquitinated proteins was controlled by Western blots.

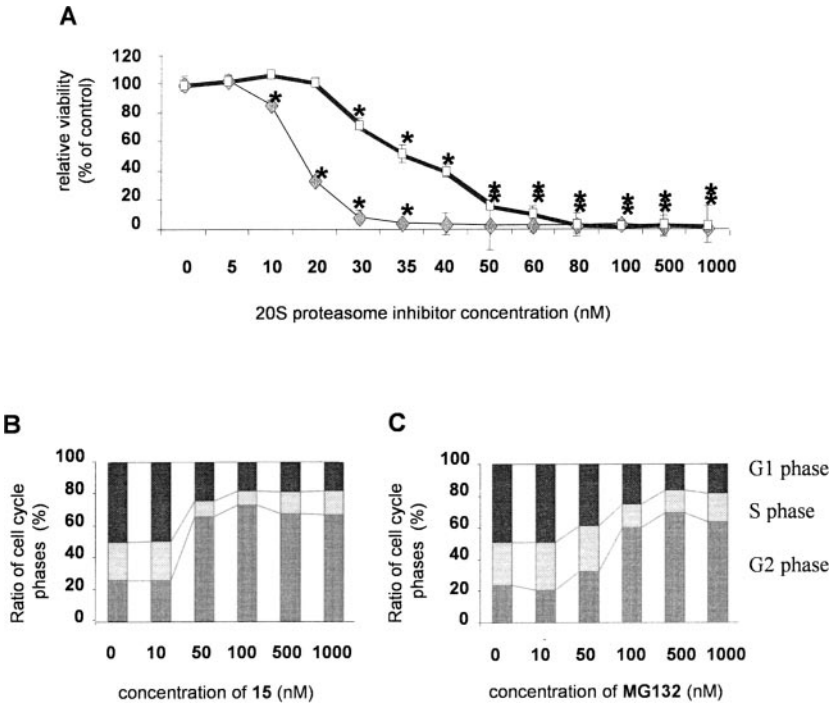

FIG. 6. **Higher susceptibility of human melanoma cells to inhibitor 15.** *A*, human melanoma cells (MeWo) were treated with increasing concentrations of inhibitor **15** or **3** (MG132) for 72 h. The viability of the cells after treatment with **15** (*gray diamonds*) or MG132 (*white squares*) was estimated by crystal violet staining. Statistical significance (*asterisks*) was calculated by Student's *t* test. *B* and *C*, investigation of cell cycle arrest. MeWo Cells were cultured with inhibitors **15** and **3** (MG132) for 24 h. The harvested cells were washed and fixed in 70% ethanol. Subsequently, the cells were incubated with RNase A. DNA was stained by addition of propidium iodide to a final concentration of 5 μg/ml. DNA was analyzed by fluorescence-activated cell sorting (FACSCalibur flow cytometer; BD Biosciences). Statistical significance was calculated by the χ^2 test. The relative distribution of cells that resided in G_1 (*black bar*), S (*white bar*), or G_2 phase (*checkered bar*) is shown for inhibitor **15** in *B* and for MG132 in *C*.

may result in the initiation of apoptosis, as reported for the proteasome inhibitor MG132 (29). Therefore, HeLa cells co-cultured with 1 μM solutions of the inhibitors **7**, **8**, **11**, **13–16**, **18**, **20–23**, and **25–28** for 24 h were monitored for the induction of apoptosis by measuring caspase 3/7 activity. Most of the tested inhibitors did not affect cell viability. In contrast, application of the inhibitors **7**, **15**, **26**, and **28** caused an activation of caspase 3/7, signaling apoptotic events (Fig. 7).

We determined the crystal structure of the yeast 20 S proteasome in complex with inhibitor **15** to reveal the inhibition mechanism of the most potent inhibitor, **15**. This compound binds in a similar orientation to the active site threonine as observed for calpain inhibitor I (6). Defined electron density was found in all active sites, indicating that compound **15** lacks subunit specificity at the high concentrations employed (10 mM). The functional aldehyde of the inhibitor forms a covalent hemiacetal bond to the Thr-1Oγ. The peptide backbone of **15** adopts a β-conformation and fills the gap between β-strands and generates an anti-parallel β-sheet structure (Fig. 8). The leucine side chain projects into the S1 pocket, whereas the P2 side chain at P2 is not in contact with the protein. The leucine side chain at P3 closely interacts with the amino acids of the adjacent β-subunit. In general, both S1 and S3 specificity pockets play a prominent role in inhibitor binding as observed in the crystal structures of the 20 S proteasome in complex with lactacystin (6) and vinylsulfone (30). The neutral character of Met-45 in subunit β5 has a dominant role for the specificity of this subunit. The crystallographic data (Fig. 8) reveal that the P1-Leu side chain of **15** causes a structural rearrangement of Met-45. In contrast to the crystal structure of the 20 S proteasome in complex with lactacystin, Met-45 is rearranged by 3 Å, avoiding a clash with the leucine side chain in P1 of **15,** thereby making the S1 pocket more spacious. Remarkably, the hydrophobic interactions between the Leu residue of the inhibitor and Met-45 are only weak, thus reducing the mean residence time of the compound at the active center. The specificity defining pockets of subunits β1 and β2 have positive and negative charges, respectively, which destabilize the protein-ligand interactions. However, the inherent reactivity of the aldehyde in compound **15** causes binding to all proteolytically active sites. These observations indicate that the functional group of this inhibitor plays the dominant role in binding.

DISCUSSION

Proteasomes are involved in a number of different cellular processes. They are important for control of the cell cycle and protect cells from apoptosis by maintaining the balance of anti-apoptotic and pro-apoptotic proteins (9, 31, 32). The interest in potent and specific inhibitors that may be used as potential drugs against cancer or neoplastic growth is very high. Here we report the synthesis of inhibitors based on the proteasomal peptide inhibitor MG132, which is a potent yet nonspecific inhibitor. We assumed that side chain modifications of the tripeptide might offer higher potency, selectivity, and site-specific inhibition of the 20 S proteasome. This assumption is based on a couple of known and potent peptidic inhibitors (16, 17, 33, 35).

All novel compounds were tested for their inhibitory capacity in cell lysates. Therefore, serine proteases, cysteine proteases, and metalloproteases were blocked by the protease inhibitor mixture Complete (Roche Applied Science) during the assay with the synthesized mimetics. The proteolysis of the hydrophobic Suc-LLVY-AMC substrate was diminished by 11 of the investigated compounds in two assays. The specific inhibition of a single catalytic site is of special interest for drug development; therefore, we analyzed the inhibition of the different proteasomal activities. The different cleavage preferences of proteasomes were determined by specific substrates for the hydrophobic (chymotrypsin-like), trypsin-like, and post-acidic (caspase-like) activities on isolated proteasomes. 12 of 22 derivatives inhibited proteasomal activities with IC_{50} values below 10 μM. The peptidic aldehydes **13** and **15** inhibited all proteasomal hydrolytic activities, whereas four compounds (**18**, **24**, **25**, and **26**) inhibited the chymotryptic and caspase-like sites. However, the purpose of this investigation was the identification of fully selective inhibitors of proteasomal activity. The tripeptidic alcohol **7** (and with lower potency, **8**) specifically reduced the trypsin-like activity, and compounds **16**, **21**, **22**, and **28** resulted in an exclusive reduction of chymotryptic

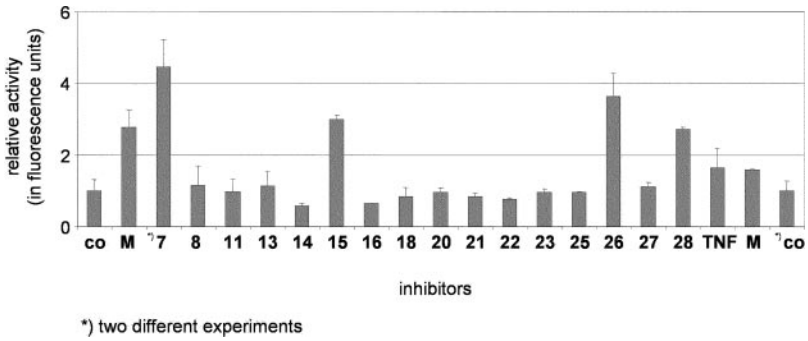

FIG. 7. **Proteasomal inhibition by 7, 15, 26, and 28 resulted in induction of apoptosis.** HeLa cells treated with 1 μM of the indicated inhibitors for 20 h were incubated with caspase substrates (Apo-One®; Promega) for 2 h. The activation of caspase 3/7 was measured at 538 nm (excitation, 485 nm). Treatment of cells with tumor necrosis factor α (*TNF*) or MG132 (*M*) served as positive controls; controls without treatment are indicated as *co*.

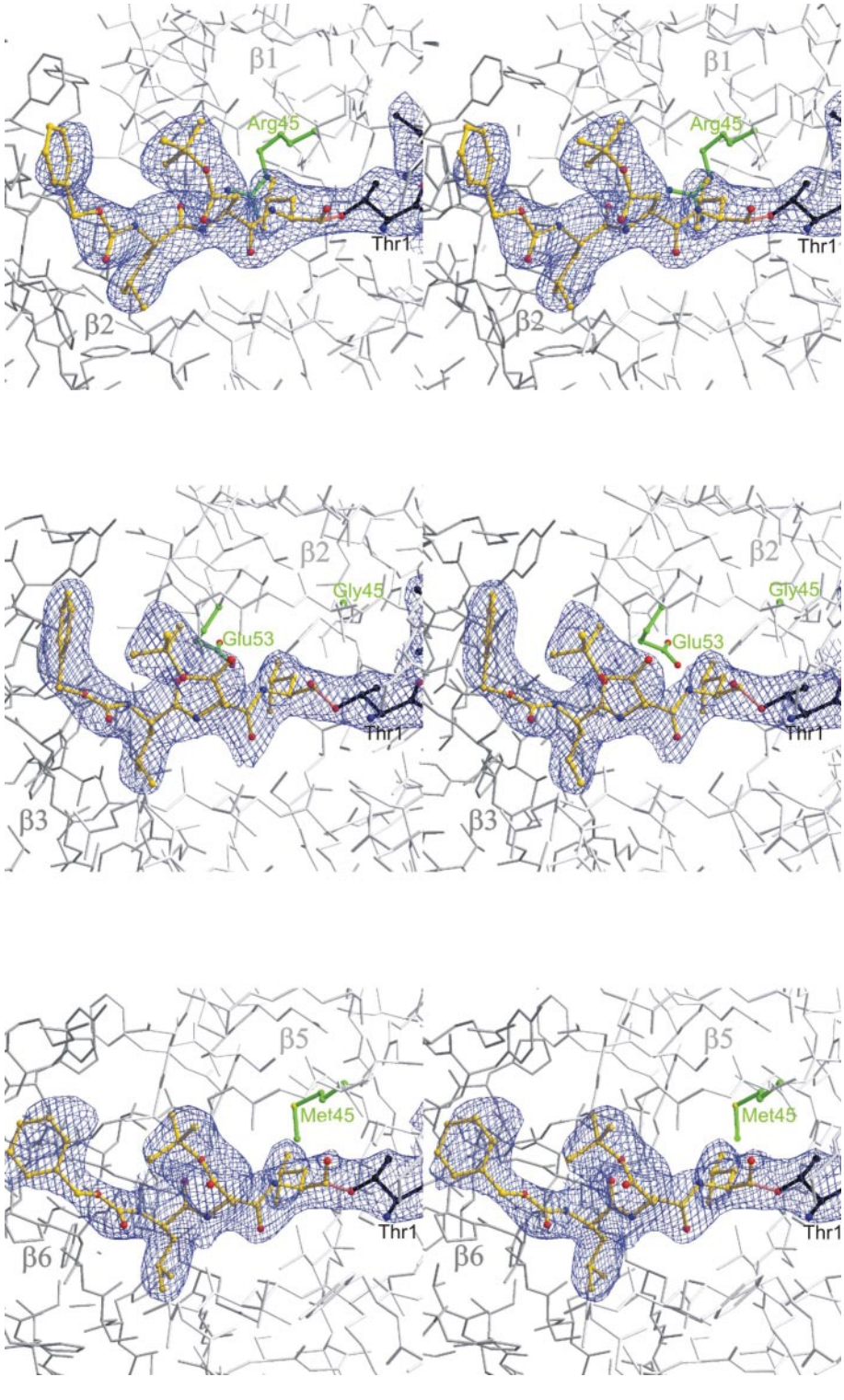

FIG. 8. **Stereoview of a 30 Å sector of the crystal structures of the (*top panel*) β1, (*middle panel*) β2, and (*bottom panel*) β5 active sites of the yeast 20 S proteasome in complex with the aldehyde 15. 15** is depicted in *yellow* and shown for each subunit with its unbiased electron density. The active site Thr-1 is highlighted in *black*, and the covalent bond between **15** and Thr-1Oγ is highlighted in *pink*. Residues that are particularly responsible for the character of the S1 subsite are drawn in *green*.

activity. Notably, the most potent of the new inhibitors feature IC_{50} values below 100 nM (**7**, **15**, and **28**). This is in the range of novel proteasomal inhibitors, which are in clinical trials (33).

Remarkably, the tetrapeptide inhibitor PSI (Z-IE(O^tBu)AL-CHO) is structurally related to our component **15** (Z-LD(O^t-Bu)L-CHO) (36), which is among the strongest inhibitors (IC_{50}, <60 nM). Moreover, it exhibited low toxicity and was able to permeate cellular membranes. The comparison of our inhibitors indicates the major contributions of the ligand side chains to the specific tight interactions with the various proteolytically active sites (Fig. 8). Similar observations were made for the alcohol derivates, with compound **7** being more effective than the other six compounds. Furthermore, very potent inhibitors were identified in the chloromethyl ketone (**22**) and in compounds **25–28**.

Tumor cells with their accelerated and neoplastic growth are often more sensitive to proteasomal inhibitors than normal cells. The clinically approved proteasomal inhibitor Bortezomib® causes growth arrest and apoptosis in the sensitive tumor cells, whereas "normal" cells tolerate higher inhibitor concentrations (37). The restriction to myeloma tumors may be overcome by more specific inhibitors, such as PSI, which blocks angiogenesis and modulates the growth of solid tumors (36). The differences in cellular features and the predictable resistance mechanisms require continuous development of new proteasomal inhibitors. Efficient cell permeation, stability in aquatic systems, and potent induction of cellular events are all mandatory for clinical applications. Therefore, we tested the permeation ability of our compounds and their *in vivo* impact on proteasomes, and we monitored the accumulation of polyubiquitinated proteins in cultured cells. A >50% reduction of cellular proteasome activity was observed for five of the new inhibitors (**15**, **22**, **25**, **26**, and **28**). The most potent inhibitions were achieved by compounds **15**, **26**, and **28**, which reduced the proteasome activity to 10% at a concentration of 1 μM. Even 50 nM solutions of compound **15** arrested 70% of the melanoma cells. Our results indicate potency, membrane permeation, and sufficient stability throughout the incubation period for the inhibitors **15**, **22**, **25**, **26**, and **28**. The cellular proteasomal activity was clearly reduced and accompanied by strong induction of apoptosis after 20 h treatment with 1 μM of inhibitors (**15**, **26**, and **28**). The prevalent enhanced sensitivity of tumor cells toward proteasomal inhibition was confirmed for inhibitor **15**. Compound **15** exerts its effects at considerably lower concentrations than MG132 and exhibits an almost identical inhibitory profile as Bortezomib®, which is characterized by a lower K_i value. The low toxicity of our new compounds and the effective proteasome inhibition encourage us to continue our evaluation of the lead compounds, **15**, **26**, and **28**.

Acknowledgment—We thank Dr. B. Dahlmann (Charité) for the gift of 26 S proteasome.

REFERENCES

1. Adams, J. (2004) *Proteasome Inhibitors in Cancer Therapy*, pp. 77–84, Humana Press Inc., Totowa, NJ
2. Glickman, M. H., and Ciechanover, A. (2002) *Physiol. Rev.* **82,** 373–428
3. Voges, D., Zwickl, P., and Baumeister, W. (1999) *Ann. Rev. Biochem.* **68,** 1015–1068
4. Peters, J. M., Cejka, Z., Harris, J. R., Kleinschmidt, J. A., and Baumeister, W. (1993) *J. Mol. Biol.* **234,** 932–937
5. Coux, O., Tanaka, K., and Goldberg, A. L. (1996) *Annu. Rev. Biochem.* **65,** 801–847
6. Groll, M., Ditzel, L., Loewe, J., Stock, D., Bochtler, M., Bartunik, H. D., and Huber, R. (1997) *Nature* **386,** 463–471
7. Baumeister, W., Walz, J., Zuhl, F., and Seemuller, E. (1998) *Cell* **92,** 367–380
8. Kloetzel, P.-M., and Ossendorp, F. (2004) *Curr. Opin. Immunol.* **16,** 76–81
9. Kloetzel, P. M. (2001) *Nat. Rev. Mol. Cell. Biol.* **2,** 179–187
10. Serwold, T., Gonzalez, F., Kim, J., Jacob, R., and Shastri, N. (2002) *Nature* **419,** 480–483
11. Seifert, U., Maranon, C., Shmueli, A., Desoutter, J.-F., Wesoloski, L., Janek, K., Henklein, P., Diescher, S., Andrieu, M., de la Salle, H., Weinschenk, T., Schild, H., Laderach, D., Galy, A., Haas, G., Kloetzel, P.-M., Reiss, Y., and Hosmalin, A. (2003) *Nat. Immunol.* **4,** 375–379
12. Golab, J., Bauer Thomas, M., Daniel, V., and Naujokat, C. (2004) *Clin. Chim. Acta* **340,** 27–40
13. An, B., Goldfarb, R. H., Siman, R., and Dou, Q. P. (1998) *Cell Death Differ.* **5,** 1062–1075
14. Orlowski, R. Z., Small, G. W., and Shi, Y. Y. (2002) *J. Biol. Chem.* **277,** 27864–27871
15. Orlowski, R. Z., Eswara, J. R., Lafond-Walker, A., Grever, M. R., Orlowski, M., and Dang, C. V. (1998) *Cancer Res.* **58,** 4342–4348
16. Kisselev, A. F., and Goldberg, A. L. (2001) *Chem. Biol.* **8,** 739–758
17. Groll, M., and Huber, R. (2004) *Biochim. Biophys. Acta* **1695,** 33–44
18. Cusack, J. C., Jr., Liu, R., Houston, M., Abendroth, K., Elliott, P. J., Adams, J., and Baldwin, A. S., Jr. (2001) *Cancer Res.* **61,** 3535–3540
19. Orlowski, R. Z., Stinchcombe, T. E., Mitchell, B. S., Shea, T. C., Baldwin, A. S., Stahl, S., Adams, J., Esseltine, D.-L., Elliott, P. J., Pien, C. S., Guerciolini, R., Anderson, J. K., Depcik-Smith, N. D., Bhagat, R., Lehman, M. J., Novick, S. C., O'Connor, O. A., and Soignet, S. L. (2002) *J. Clin. Oncol.* **20,** 4420–4427
20. Paramore, A., and Frantz, S. (2003) *Nat. Rev. Drug Discov.* **2,** 611–612
21. Myung, J., Kim, K. B., and Crews, C. M. (2001) *Med. Res. Rev.* **21,** 245–273
22. Schmidt, B. (2003) *Chembiochem.* **4,** 366–378
23. John, V., Beck, J. P., Bienkowski, M. J., Sinha, S., and Heinrikson, R. L. (2003) *J. Med. Chem.* **46,** 4625–4630
24. Leslie, A. G. W. (1994) *Mosflm User Guide, Mosflm Version 5.20*, MRC Laboratory of Molecular Biology, Cambrige, UK
25. Brünger, A. T. (1992) *X-PLOR, Version 3.1. A System for X-ray Crystallography and NMR*, Yale University Press, New Haven, CT
26. Turk, D. (1992) *Weiterentwicklung eines Programms für Molekülgraphik und Electronendichte-Manipulation und seine Anwendung auf verschiedene Protein-Strukturaufklärungen.* Ph.D. thesis, Technische Universität München, Munich
27. Engh, R., and Huber, R. (1991) *Acta Crystallogr.* **A47,** 392–400
28. Schmidt, B., Ehlert, D. K., and Braun, H. A. (2004) *Tetrahedron Lett.* **45,** 1751–1753
29. Guzmen, M. L., Swiderski, C. F., Howard, D. S., Grimes, B. A., Rossi, R. M., Szilvassy, S. J., and Jordan, C. T. (2002) *Proc. Natl. Acad. Sci. U. S. A.* **99,** 16220–16225
30. Groll, M., Nazif, T., Huber, R., and Bogyo, M. (2002) *Chem. Biol.* **9,** 655–662
31. Ling, Y. H., Liebes, L., Ng, B., Buckley, M., Elliott, P. J., Adams, J., Jiang, J. D., Muggia, F. M., and Perez-Soler, R. (2002) *Mol. Cancer Ther.* **1,** 841–849
32. Meiners, S., Heyken, D., Wellej, A., Ludwig, A., Stangl, K., Kloetzel, P.-M., and Krüger, E. (2003) *J. Biol. Chem.* **278,** 21517–21525
33. Adams, J. (2004) *Nat. Rev. Cancer* **4,** 349–360
34. Garcia-Echeverria, C., Imbach, P., France, D., Fürst, P., Lang, M., Noorani, A. M., Scholz, D., Zimmermann, J., and Furet, P. (2001) *Bioorg. Med. Chem. Lett.* **11,** 1317–1319
35. Traenker, E. B., Wilk, S., and Baeuerle, P. A. (1994) *EMBO J.* **13,** 5433–5441
36. Stoklosa, T., Golab, J., Wojcik, C., Wlodarski, P., Jalili, A., Januszko, P., Giermasz, A., Wilczynski, G. M., Pleban, E., Marczak, M., Wilk, S., and Jakobisiak, M. (2004) *Apoptosis* **9,** 193–204
37. Hideshima, T., Richardson, P., Chauhan, D., Palombella, V. J., Elliott, P. J., Adams, J., and Anderson, K. C. (2001) *Cancer Res.* **61,** 3071–3076